Design and Fabrication of Two-Dimensional Superconducting Bolometer Arrays

Dominic J. Benford[† a], Johannes G. Staguhn[a,b], Gordon J. Stacey[c], Lyman A. Page[d], S. Harvey Moseley[a], Kent D. Irwin[e], James A. Chervenak[a], Christine A. Allen[a]

a NASA / Goddard Space Flight Center, Greenbelt, MD 20771 USA
b SSAI, Lanham, MD 20706 USA
c Cornell University, Ithaca NY 14853 USA
d Princeton University, Princeton NJ 08544 USA
e NIST / Boulder, Boulder, CO 80305 USA

ABSTRACT

We have been developing an architecture for producing large format, two-dimensional arrays of close-packed bolometers, which will enable far-infrared to millimeter wavelength (λ=100 μm–2 mm) cameras and spectrometers to obtain images and spectra orders of magnitude faster than present instruments. The low backgrounds achieved in these instruments require very sensitive detectors with NEPs ranging from 10^{-17} to 10^{-19} W/√Hz. Superconducting transition edge sensor bolometers can be close-packed using the Pop-Up Detector (PUD) format, and SQUID multiplexers operating at the detector base temperature can be intimately coupled to them. The array unit cell is 8×32 pixels, using 32-element detector and multiplexer components. We have fabricated an engineering model array with this technology featuring a very compact, modular approach for large format arrays. We report on the production of the 32-element components for the arrays. Planned instruments using this array architecture include the Submillimeter and Far-InfraRed Experiment (SAFIRE) on the SOFIA airborne observatory, the South Pole Imaging Fabry-Perot Interferometer (SPIFI) for the AST/RO observatory, the Millimeter Bolometer Camera for the Atacama Cosmology Telescope (MBC/ACT), and the Redshift "*Z*" Early Universe Spectrometer (ZEUS).

Keywords: bolometer array, superconducting transition edge sensor, SQUID multiplexer, SOFIA, AST/RO, ACT

1. INTRODUCTION

Far-infrared and submillimeter instruments being fabricated for ground-based and airborne observations require arrays of broadband detectors containing several hundred elements. The state-of-the-art is currently the 384-pixel arrays manufactured at NASA's Goddard Space Flight Center for the CSO/SHARC-II and SOFIA/HAWC instruments[1]. These arrays use a design for close-packing detectors to achieve a near unity filling factor. However, these arrays use semiconducting thermistors read out by individual FETs for every pixel. We have several applications that require detectors with many more pixels, and sensitivity at least 100 times better. A new design using superconducting detectors and multiplexed SQUID readouts can achieve this.

Three far-infrared spectrometers and one camera have been proposed: SAFIRE on SOFIA, SPIFI on AST/RO, ZEUS on the JCMT, and MBC on ACT. The Submillimeter and Far-InfraRed Experiment (SAFIRE) on the SOFIA airborne observatory is designed to be a wide-field imaging spectrometer with moderate spectral resolving power[2]. It will achieve a resolution of about 300 km/s, continuously tunable over the 145 μm-655 μm range. Combining the low background present at the high altitude of the observatory with the bandwidth narrowing yields a requirement for a detector as or more sensitive than any yet made at this wavelength. Additionally, the requirement for a wide field of view demands an array containing hundreds of pixels. SPIFI (South Pole Imaging Fabry-Perot Interferometer) is a high resolution (up to 30 km/s) Fabry-Perot spectrometer for operation in the bands available from the ground, particularly 200 μm and

† Corresponding Author: Dominic J. Benford; dominic.benford@gsfc.nasa.gov; 301.286.8771; Code 685, NASA/GSFC, Greenbelt, MD 20771; http://lasp-nts1.gsfc.nasa.gov/irbranch/Dominic_J_Benford.html

Millimeter and Submillimeter Detectors for Astronomy II, edited by
Jonas Zmuidzinas, Wayne S. Holland, Stafford Withington, Proceedings of
SPIE Vol. 5498 (SPIE, Bellingham, WA, 2004) · 0277-786X/04/$15 · doi: 10.1117/12.552108

350 μm[3]. The MBC (Millimeter Bolometer Camera) on the Atacama Cosmology Telescope[4] is to be a dedicated survey instrument, using three bands between 1.1 and 2.0 mm to produce sensitive images of the Sunyaev-Zel'dovich effect. ZEUS is a grating spectrometer with resolution approaching that of SAFIRE[5]. To within a factor of a few, all these arrays require similar sensitivity. SAFIRE will feature a 16×32 array to fill its field of view; ZEUS requires only an 8×32 array, and SPIFI could use either format. The MBC requires three similar arrays of 32×32 format apiece, the most challenging development.

The largest array of detectors for far-infrared wavelengths has been built for the HAWC and SHARC-II instruments[6], each containing 384 semiconducting bolometers operating at ~200 mK coupled to 384 JFET amplifiers operating at ~120 K. The mechanical, thermal, and optical design of this array is a challenging engineering exercise. In order to simplify this, instead of a semiconducting thermistor, a superconducting transition edge sensor (TES) can be used to read out the detector temperature. A TES bolometer has a faster response time than an identically designed, same-sensitivity semiconducting bolometer (or a more sensitive bolometer for the same response time) due to the strong negative electrothermal feedback intrinsic in a voltage-biased TES[7]. TES bolometers are inherently low impedance devices, so they are well matched to being read out by DC SQUID amplifiers[8]. These amplifiers have a large noise margin over the TES Johnson noise and bolometer phonon noise. This permits the bolometer to be read out in a multiplexed fashion by a suitable SQUID multiplexer[9], thereby reducing the amplifier size and the wire count. Because SQUID multiplexed amplifiers operate at the base temperature of the bolometer, they can be coupled very closely, removing the complex interfaces necessary with semiconducting bolometers. In light of these advantages, we have engaged in the production of arrays of multiplexed superconducting bolometers for SAFIRE, SPIFI, MBC, and ZEUS.

2. DETECTOR ARRAY REQUIREMENTS

In order to produce detectors with absorption efficiency at wavelengths of 2 mm, it is necessary to set the pixel scale to at least 1 mm. The spectral resolving power of SAFIRE and SPIFI is generated by a high-resolution Fabry-Perot with an order-sorting Fabry-Perot and broadband filters. A convenient beamsize to propagate through such optical setups would be ~50 mm in diameter, which, for a resolving power of 300 km/s, yields a maximum field of view of 6′ diameter on SOFIA. This field would contain about 1000 pixels of 10″ square, but in an inconvenient distribution on the focal plane. We have instead chosen to use a 32-element multiplexer that couples to a linear detector array that is conveniently close to the field size. The maximum array format that fits within this 6′ diameter is then a 16×32 array, assuming closely packed detectors. The MBC has a large field of view, and so requires a 32×32 array, based in part on the availability of the 32-element technology.

All these instruments operate in a suborbital environment, where the atmosphere is the dominant source of background power on the bolometers. Figure 1 shows the expected atmospheric emissivity for the applications being considered. This can be translated into an atmospheric photon noise equivalent power (NEP), as shown in Figure 2. In all cases, a detector with pixel size appropriate to Nyquist-sampled spacing at the shortest wavelength of operation is assumed, and with the relevant spectral resolutions and reasonable optical efficiencies included. The SOFIA/SAFIRE detectors will need to achieve a phonon and Johnson noise sum of $<3\cdot10^{-19}$ W/√Hz in order to be background-limited, and must be able to absorb up to ~0.3 pW in order to avoid saturation. This puts a stiff requirement on the dynamic range of the bolometers, in that the ratio of maximum power detected to the minimum power detectable in unity bandwidth is about 10^6.

3. DESIGN OF CLOSE-PACKED ARRAY

Bolometers require very low thermal conductance supports in order to make them sensitive. These supports are usually long, thin wire-like structures that operate in tension and occupy appreciable focal plane area, often being larger in area than the optically active portion of the bolometer itself. Along with these supports, wiring is needed to connect to the bias and readout circuitry; this is often another space-consuming portion of an array. Substantial effort at NASA's Goddard Space Flight Center has gone into the development of an approach that brings the mechanical and electrical connections out behind the bolometer, permitting all the necessary connections while occupying the minimum focal plane area possible. A rectangular bolometer absorber is manufactured in a thin silicon or silicon nitride membrane with four legs projecting out of the sides. These legs are folded beneath the absorber, forming a table-like structure with the supports under flexural rather than tensile stress. This approach is referred to as a "Pop-Up Detector" or PUD, by analogy to the deployment of similar structures in children's books.

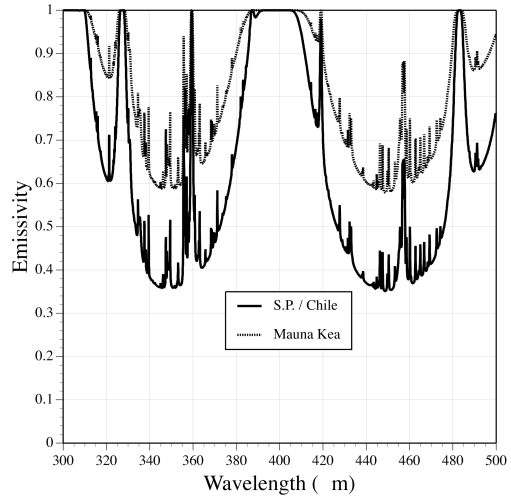

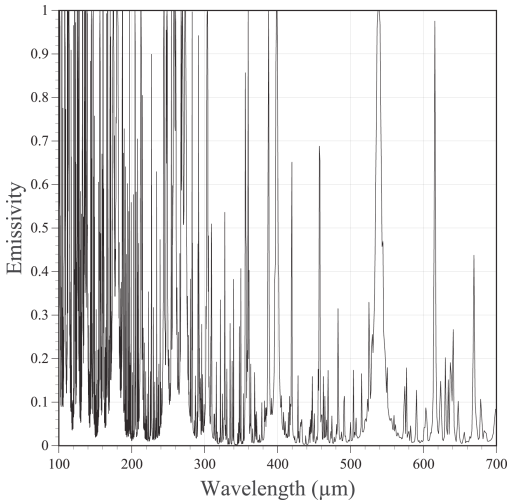

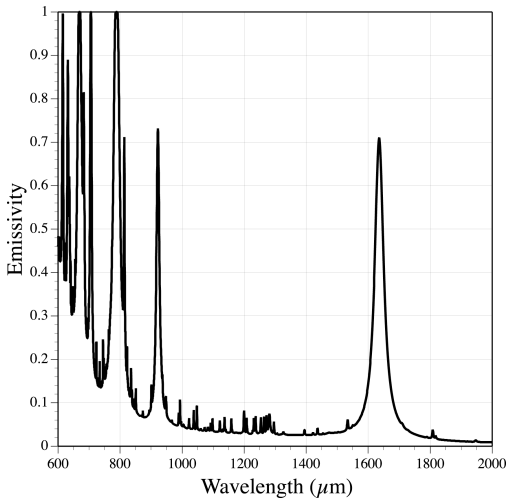

Figure 1. Atmospheric emission[10] from: (top) the ground using ZEUS and SPIFI at Mauna Kea, the South Pole, or Chile, assuming typical precipitable water vapor (middle) SOFIA altitudes, with 5μm PWV; (bottom) Chile for the ACT.

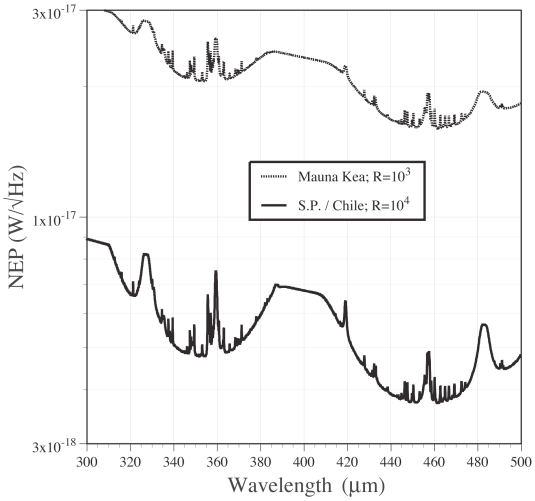

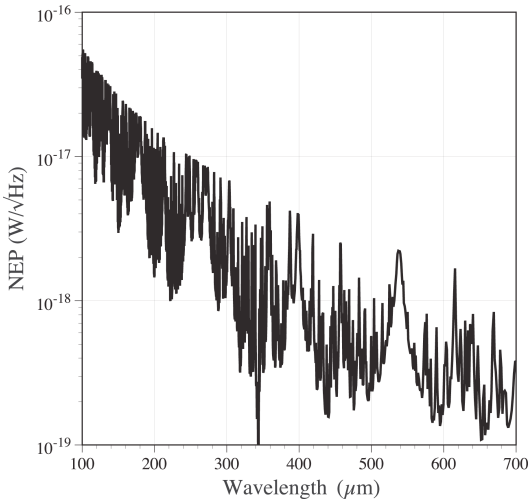

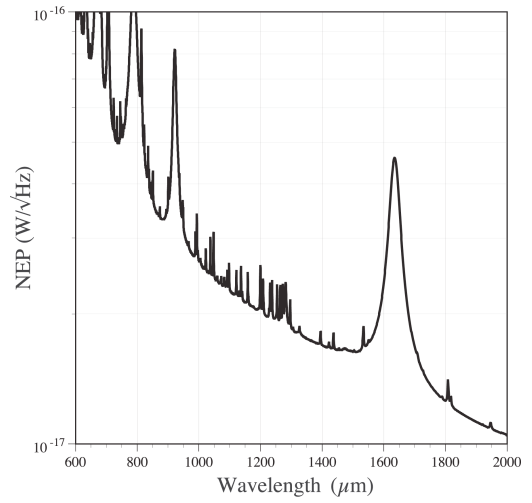

Figure 2. Photon noise equivalent powers from the emission shown in Figure 1, using a spectral resolution and optical efficiency appropriate to each instrument.

The first large-scale PUD array has been built for the SHARC-II instrument on the Caltech Submillimeter Observatory and the HAWC instrument on SOFIA[1] (Figures 3 & 4). Both of these feature 12×32 bolometers using semiconducting thermistors, and will operate in broadband imaging cameras. These arrays have demonstrated the folding, stacking, and interconnection procedures necessary to make a close-packed array. Because of the much simpler thermal and mechanical interfacing possible with superconducting bolometers, we have redesigned the PUD assembly to produce an architecture that permits very compact, close-packed arrays of multiplexed superconducting TES bolometers.

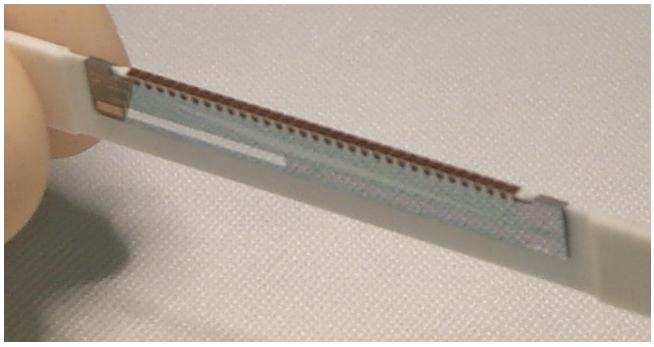

Figure 3. Photo of a folded 32-element array for the HAWC and SHARC-II instruments.

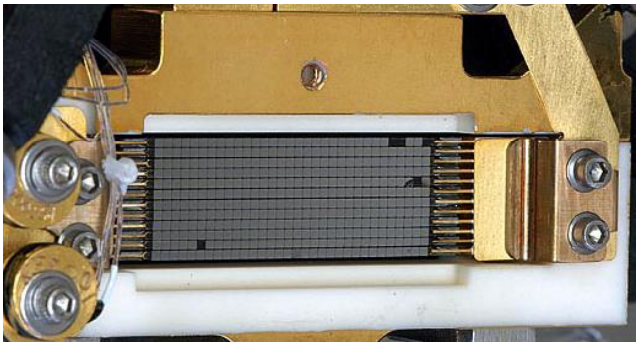

Figure 4. Photo of the assembled 12x32-element array for the SOFIA/HAWC camera[11].

4. INDIVIDUAL BOLOMETER DESIGN

A TES bolometer is fundamentally no different from a semiconducting bolometer, other than a change in the thermistor that has substantial implications. Infrared light is absorbed in the bolometer and converted into heat, warming the detector of heat capacity C above its nominal temperature T_{bias} (Figure 5). This temperature change is converted into a resistance change which is measured electrically. The heat is conducted away through a thermal conductance G to a heat sink at T_{bath}. A superconducting transition at temperature T_C yields an extremely sharp but continuous change in resistance from near zero to the normal state resistance (Figure 6). A unitless measure of the sharpness of the transition is defined as the sensitivity α:

$$\alpha \equiv \frac{d\log R}{d\log T} = \frac{T}{R}\frac{dR}{dT} \approx \frac{2T_C}{\Delta T}$$ where ΔT is the approximate transition width.

It has been found that transitions with higher α typically have higher excess (above phonon) noise[12,13]. The sensitivity can be changed by adjusting the quantity, location, and orientation of normal metal bars added onto the TES, as shown at bottom in Figure 6.

The response time of a bolometer is typically the thermal time constant, $\tau = C/G$. However, TES bolometers can be faster than this by means of electrothermal feedback. When biased onto the transition, power is dissipated in the thermistor as $P=V^2/R$. When optical power is applied, the thermistor warms up, increasing its resistance dramatically. The bias power drops (since the bias voltage is held constant), bringing the TES back towards the stable bias point. The effective time constant is then approximately $\tau_{eff} = \tau n/\alpha$, where n is the temperature index of the thermal conductance. Additionally, at low frequencies ($(\omega\tau_{eff})^2 \ll 1$), the Johnson noise is suppressed through the action of the electrothermal feedback by a factor of $(n/\alpha)^2$. The end result of this is that the intrinsic noise of a TES bolometer is typically dominated by the phonon noise alone.

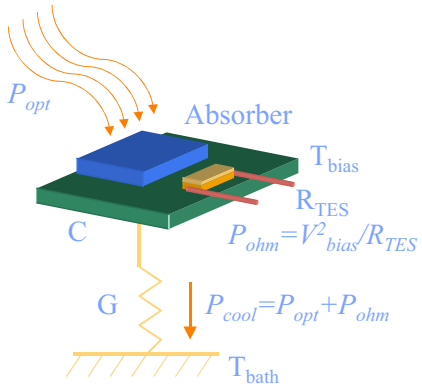

Figure 5. Operation of a TES bolometer.

Superconducting transitions can be made in several ways. In order to produce a thermistor with a tunable T_C and with a known resistance, we manufacture superconducting-normal bilayers. The superconductor, in this case a thin film of molybdenum, has its transition temperature reduced by proximity to a thin film of a normal metal such as gold or copper. This process is described more fully by Chervenak et al.[14]. The thermistor is manufactured by deposition and photoetching to produce a small (50μm × 100μm × 0.1μm) active volume.

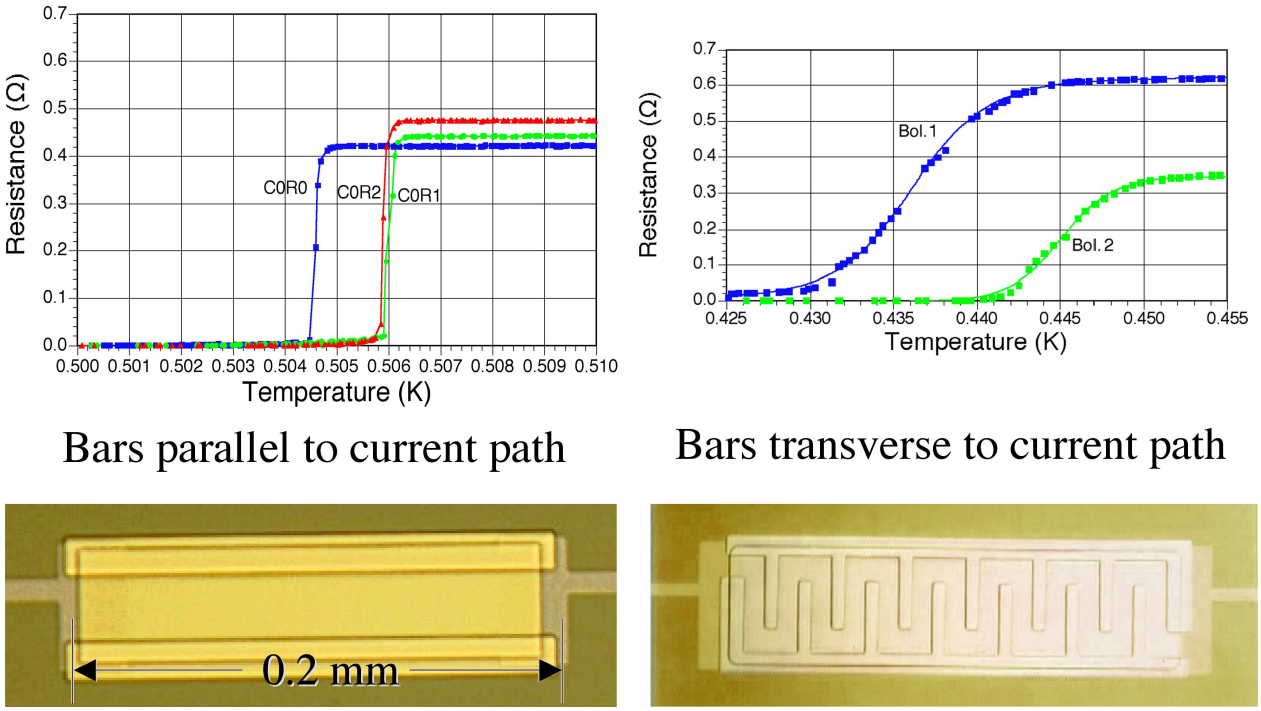

Figure 6. Resistance as a function of temperature for several devices of slightly different TES geometries, including normal metal bars for noise suppression. A marked difference in the sharpness of the transition is seen between those devices having bars oriented transverse to the current flow versus those normal to the current flow. Lower sharpness correlates with lower noise.

The voltage-current characteristic of a TES bolometer is quite different from that of a semiconducting bolometer. If we consider a voltage-biased TES cooling down from the normal state, the device exhibits a constant resistance ($I=V/R$) (Figure 7). For an ohmic device, this obviously will result in linear response all the way to zero bias. For a superconducting TES, as we lower the bias voltage, at some point the bias power becomes too little to keep the device in the normal state, and it will begin to drop in resistance. Because the transition width is small, the TES is nearly isothermal at any point on the transition, and so the total dissipated power must be constant. In this case, the current becomes a hyperbolic function of the voltage, $I=P/V$. At some point, the bias current reaches a maximum value (set by electronics) and the TES becomes superconducting. The responsivity of a TES on its transition is approximately $1/V$ (A/W).

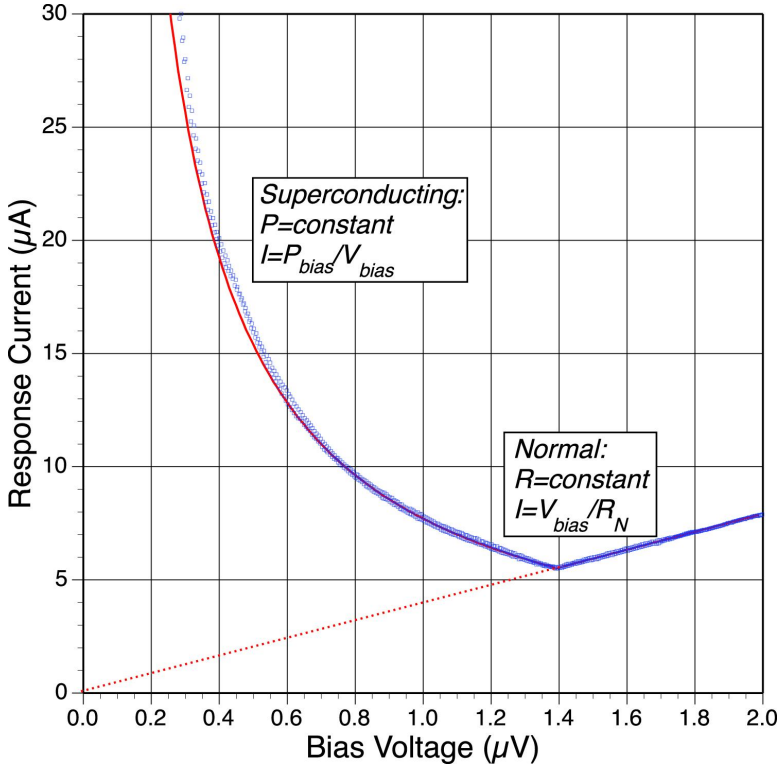

Figure 7. Voltage-current characteristic of an ideal superconducting transition edge sensor (solid line) compared with measurements from a detector (points).

The NEP of a phonon-noise-limited superconducting bolometer can be calculated easily ($NEP_{phonon} = \sqrt{2kT_C^2 G}$, given a thermal conductance $G(T)$). For a superconducting TES, the detector will saturate when the combined optical (P_{opt}) and electrical bias (P_{elect}) power exceed the power thermally conducted away by the bolometer supports:

$$P_{opt} + P_{elect} \geq \int_{T_{\text{sink}}}^{T_c} G(T)dT ,$$

where T_c and T_{sink} are the transition temperature and the thermal sink temperature, respectively. The GSFC bolometer design[15] using micromachined silicon nitride structures can yield a thermal conductance of $G(T) \approx 5 \cdot 10^{-11}\ T^3$ W/K (e.g., the bolometer shown below in Figure 8). Such a detector could be used for the broadband spectrometer SOFIA/SAFIRE, since the phonon-limited NEP of such a bolometer is $1 \cdot 10^{-19}$ W/$\sqrt{\text{Hz}}$ at a transition temperature of around 0.1K. When biased suitably, the maximum saturation power is obtained with negligible electrical power and a sufficiently low sink that its temperature is unimportant: $P_{sat} = 1.25 \cdot 10^{-11}\ T_c^4$ W.

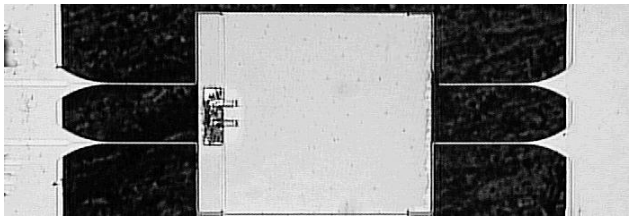

Figure 8. Photo of a single bolometer manufactured using photolithographic techniques in a silicon nitride membrane, showing the slender mechanical supports that yield low thermal conductance to the 1mm^2 absorber. The superconducting thermistor is the small rectangle at the left edge of the bolometer.

5. INCREASING DYNAMIC RANGE

We assume a generic TES bolometer with a thermal conductance $G(T) = G_1 T^{\xi}$ derived from mechanical isolation or electron-phonon decoupling. The saturation power for this bolometer is:

$$P_{saturation} \equiv \int_{T_{bath}}^{T_{C1}} G(T)\ dT \approx \frac{G_1\ T_{C1}^{\xi+1}}{\xi+1} \tag{1}$$

assuming that the bath temperature T_{bath} is small compared to the transition temperature T_{C1}. The phonon noise equivalent power is also related to this thermal conductance:

$$NEP_{phonon} = \sqrt{2kT^2\overline{G}} \approx \sqrt{2kT_{C1}^{\xi+2}\frac{G_1}{\xi+1}}. \tag{2}$$

If we define the dynamic range $\Re$ to be the ratio of the saturation power to the NEP, this figure of merit becomes:

$$\Re \equiv \frac{P_{saturation}}{NEP_{phonon}} = \sqrt{\frac{G_1}{2k(\xi+1)} \cdot T_{C1}^{\xi}} \text{ and therefore } \Re = \sqrt{\frac{P_{saturation}}{2kT_{C1}}} = \frac{NEP_{phonon}}{2kT_{C1}}.$$

For a bolometer optimized for a given background-limited noise performance or for a given maximum background power, lowering the transition temperature will improve the dynamic range. However, the design requirement of the low background with large wavelength coverage of SOFIA/SAFIRE will push the noise performance while still requiring high saturation powers. Consistent with this goal, equations (1) and (2) show that the dynamic range can be improved by increasing the geometric factor G_1 and lowering T_{C1} to compensate.

An alternative approach is to produce a device with an adjustable transition temperature. In the simplest implementation, two TES devices would be placed in series, both isolated by the same thermal conductance. If the second device has a transition temperature $T_{C2} > T_{C1}$, the dynamic range becomes:

$$\Re_{two-T_C} = \frac{\int^{T_{C2}} G(T)\ dT}{NEP_{phonon}} = \sqrt{\frac{G_1}{2k(\xi+1)} \cdot \frac{T_{C2}^{2\xi+2}}{T_{C1}^{\xi+2}}} = \left(\frac{T_{C2}}{T_{C1}}\right)^{\xi+1} \cdot \Re .$$

If the transition temperature ratio is 4 and the thermal isolation is provided by a dielectric material of $\xi \approx 3$, the two-T_C detector provides an increase of 256 times the dynamic range. A two-T_C device with a temperature ratio of 10 could provide a 10^4 improvement in dynamic range. The disadvantage of this approach is that it reduces the phonon noise margin over photon noise by a factor of $(T_{C2}/T_{C1})^{1/2}$. However, this is not a complex device to fabricate and might be easily implemented with a small heater on every bolometer. Direct pixel heating is being investigated for improving DC stability for the SCUBA-II detector arrays[16]. Despite some complexities, increasing the usable dynamic range of TES bolometers can save substantial cost in the detectors and electronics if multiple separately optimized arrays were used. Test investigations of a two-T_C bolometer have been carried out, demonstrating the feasibility of this approach[17].

6. 32-ELEMENT LINEAR ARRAY DESIGN

When designing an array using the PUD architecture, the basic component is one of the first choices to make. We have chosen to use linear arrays of 32 detectors, primarily due to the fact that present technology makes possible a 32-input SQUID multiplexer, built at NIST-Boulder. We have manufactured 32-element linear arrays of 1mm^2 pixels (Figure 9) with appropriate thermal conductances for use in low background instruments at ~0.1K temperatures, although the transition temperature was set to 440mK for convenience of early testing with a ^{3}He refrigerator[18]. SAFIRE's adiabatic demagnetization refrigerator will provide a 60mK base temperature, while ACT, SPIFI and ZEUS will use ^{3}He refrigerators operating at ~250mK.

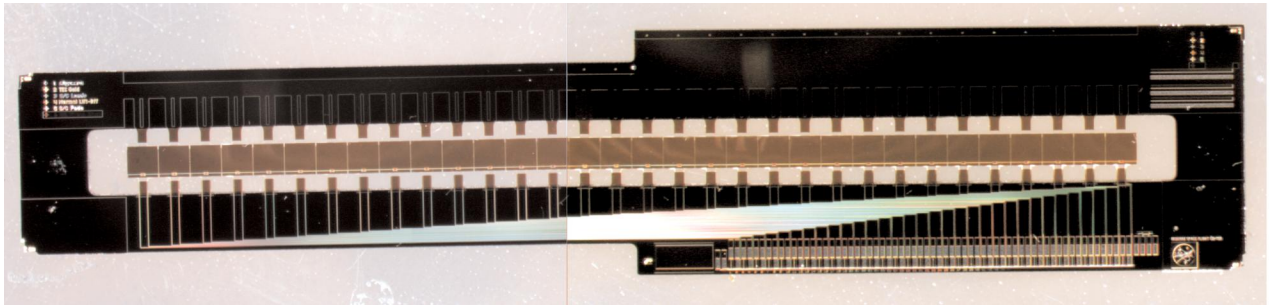

Figure 9. Photo of a 32-element linear array of superconducting bolometers. Each pixel is 1mm on a side and is suspended by four legs to allow folding. The superconducting bilayer is the rectangle near the bottom edge of each pixel.

The 32-element PUD array for SAFIRE is designed as an extension of the SHARC-II and HAWC arrays. New features include alignment holes and wiring with on-chip bias resistors (Figure 10). Because these resistors are low value – typically a few mΩ – it is useful to use photolithography to yield the resistance precision necessary in a small size. The bond pads are arranged so that each detector has a bias shunt resistor, but ganged together in series to deliver the same bias to all detectors (Figure 11). When the 32-element detector array is folded, the alignment holes permit several of them to be stacked together on dowel pins to produce a single two-dimensional array.

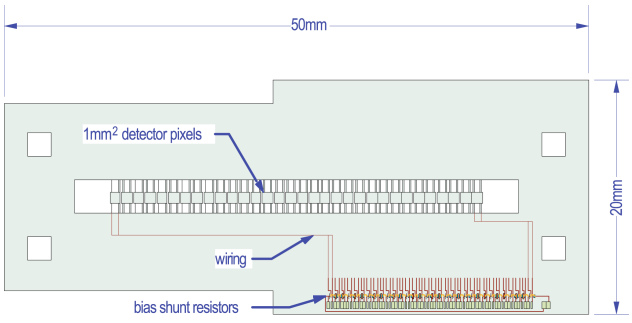

Figure 10. Layout of a 32-element array with on-chip bias circuitry and assembly alignment holes.

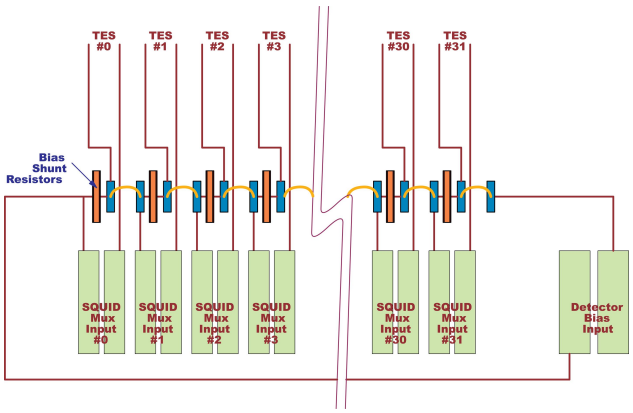

Figure 11. Layout of bond pads on the detector chip, showing circuitry for the bias shunt resistors.

7. 32-ELEMENT SQUID READOUT

Individual SQUID amplifiers are adequate for reading out small numbers of TES elements. However, large-scale, two-dimensional arrays of cryogenic bolometers present several challenges for their readout. The wire count and power dissipation scale linearly with pixel count in a nonmultiplexed implementation. Multiplexed SQUID amplifiers can be used to reduce these and other problems associated with scaling. While there is some complexity involved in developing multiplex technology, this burden is balanced by the alternative burden of the mechanical/electrical complexity of wiring an individual SQUID readout per detector. As a collaborative effort between NASA-Goddard and NIST-Boulder we have, over the past few years, made substantial progress in the use of SQUID multiplexers for the readout of low-impedance devices. An eight-input SQUID multiplexer/amplifier[9] has been used to demonstrate Johnson-noise-limited readout[19], detection of infrared light with TES bolometers[20], and operation in an astronomical application[21]. There is now a 32-input SQUID multiplexer with a more advanced architecture[22]. A simplified block diagram of this system is shown in Figure 12, illustrating the system for this multiplexer. We describe the operation of the multiplexer itself below.

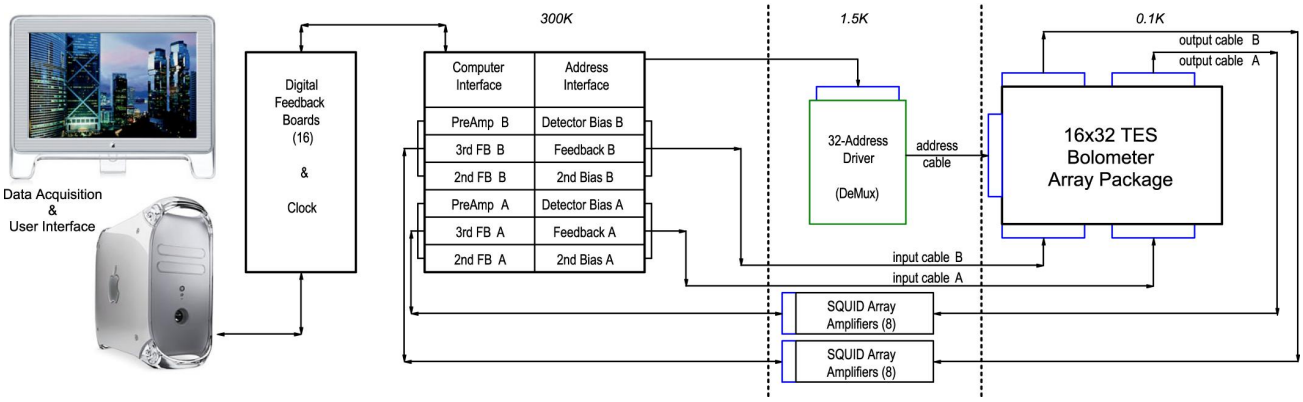

Figure 12. Simplified block diagram for a 16x32 bolometer array data acquisition system.

With a multiplexed array of detectors, each bolometer is coupled to a dedicated first stage SQUID amplifier. These first stage amplifiers are configured in a column format, with 32 inputs per column (Figure 13). The signals from all 32 SQUIDs in the column are summed and coupled to a second stage amplifier. Since only one first stage SQUID is on at a time, the signal from the corresponding bolometer is the only signal presented to the second stage amplifier. The other first stage SQUIDs remain in a superconducting state, contributing no signal or noise and dissipating no power. By sequentially turning on the first stage amplifiers, the single output channel per column of detectors carries a time-domain-multiplexed signal with all the signals from the 32 bolometers. The address lines for every row of first stage SQUIDs are wired in series from column to column, so only one set of address lines is required per row of the two dimensional array. Each SQUID is shunted with an address resistor of similar impedance ($R_A \approx 1\ \Omega$) and the pair is biased with a constant current, yielding a SQUID that is neither voltage nor current biased.

The second stage SQUIDs are voltage biased, and couple to a 100-element series array of SQUIDs at a higher temperature (Figure 14), which in turn couples to room-temperature electronics. Custom digital electronics are used to process signals from each column, control the timing of the row multiplexing, and apply a switched feedback signal to a common feedback line for each column. Further details of these electronics can be found elsewhere in this volume[23]. The address current is switched from one row to the next at the *line rate*, while the full array is sampled at the *frame rate*, which is 32 times slower than the line rate. This multiplexer architecture has received extensive laboratory testing, and has been found to work well. It can operate at rapid (>MHz) switching rates with low channel-to-channel crosstalk.

To complete the description of the schematic in Figure 13 a 32-element integrating inductor needs to be included. The purpose of this inductor is to provide a bandpass filter on the TES circuit, which serves to integrate the TES signal. This results in the multiplexer being used to sample an already integrated signal, rather than merely integrating 1/32 of the time per channel. For noise purposes, the sampling time of the SQUID is shorter than that of the TES, so the SQUID noise must be smaller (by a factor of at least $1/\sqrt{32}$) than the noise of the input.

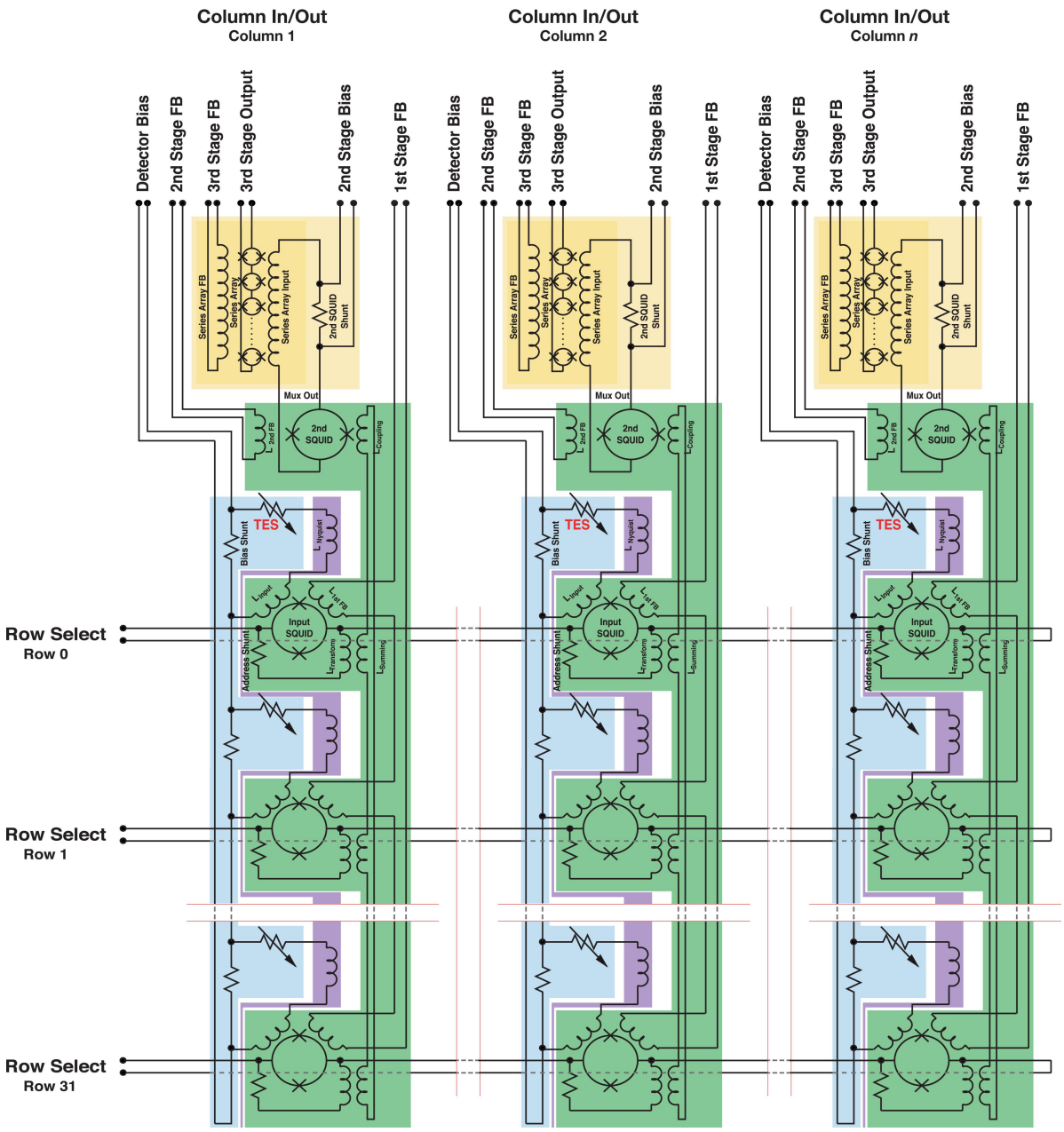

Figure 13. Schematic of a n×32-element readout circuit comprised of sets of 32-element TES bolometer arrays coupled to 32-element SQUID multiplexers, with 32-element integrating (Nyquist) inductors; each column of 32 elements is amplified by a 100-element SQUID amplifier. This amplifier is housed in a separate enclosure and can be operated at a higher temperature than the bolometers.

Figure 14. (Left) Single 100-element SQUID array chip. (Right) daughterboard and motherboard for holding eight such chips in a connectorized, magnetically shielded enclosure around 1cm × 3cm × 6cm in size.

8. TWO-DIMENSIONAL ARRAY ASSEMBLY

The assembly of a superconducting PUD array is designed to require very little difficult craftsmanship, provided that the individual detectors and SQUID multiplexers have been previously characterized and prepared. A folded PUD array and a circuit board carrying the SQUID multiplexer and Nyquist inductor is first installed on a baseplate, using alignment features to position them correctly. Wirebonds connect the detector to the readout. The circuit board fans out to a set of cables attachments, providing for all the electrical connections. A second PUD array and circuit board is then added atop the first, but this set is mirror-imaged such that the bond pad areas do not overlap each other. This permits space for wirebonds without the fear that subsequent stacked layers will crush the fragile interconnections. The process continues until all 8, 16, or 32 of the PUD arrays and circuit boards are installed. At this point, cabling for all the readouts would be dangling to the sides. A mechanical model (without cabling) was built to test the assembly process (Figure 15). To complete the array fabrication, a separate circuit board to carry the input SQUID addressing and readout connections is used. The reason for this is that while the readouts are organized per-column, the addressing is a common bus to all columns. Each column must attach to the address bus in series. This address bus ensures that all columns turn on their input SQUIDs simultaneously with the minimum number of wires. The finished PUD array is mounted by means of a thermally isolating kinematic Kevlar suspension (Figure 16)

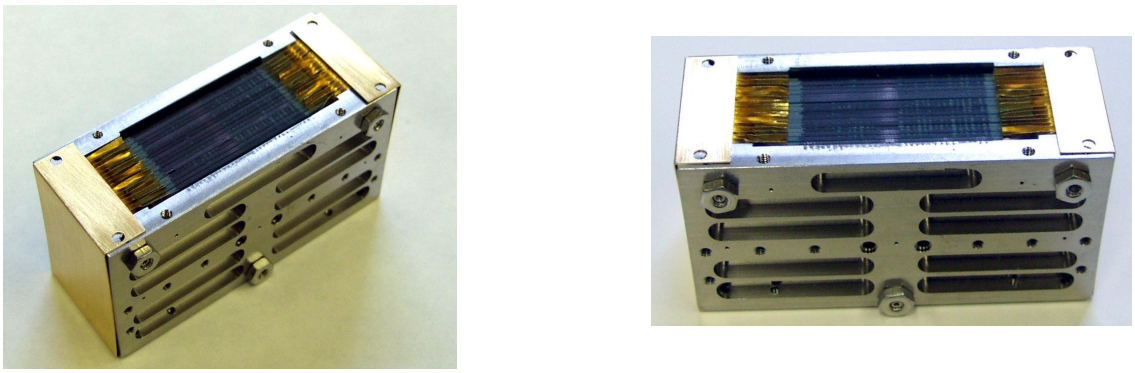

Figure 15. A mechanical prototype 16×32 array stack; a complete array would also have wires attached to the circuit boards to make electrical connections, which are brought of the light-tight package through baffles to connectors mounted on the rear.

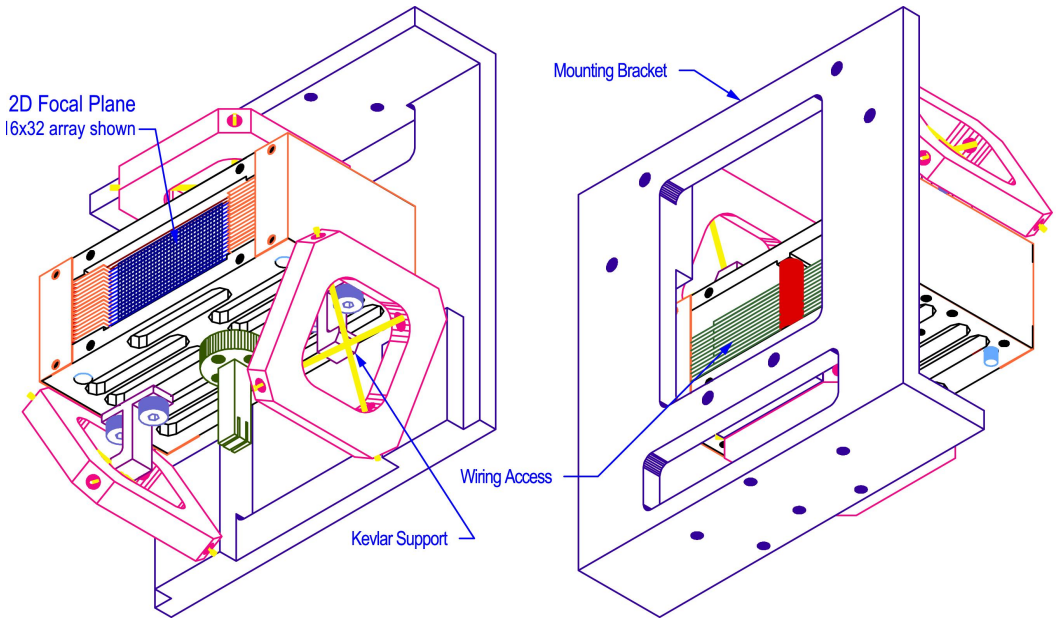

Figure 16. Completed detector array package, showing mechanical and thermal attachments but not the electrical connectors. The cold detector package is mounted by a mechanically stiff yet thermally isolating support, using a kinematic Kevlar suspension[24].

9. SUMMARY

We have designed kilopixel arrays of superconducting TES bolometers with integrated SQUID multiplexers for a variety of suborbital applications. Prototype detectors have been manufactured and tested in a 300mK setup. These detectors have shown good performance and behave according to theory. The electrical circuit has been designed with the goal of making a compact, low power multiplexed readout that can be intimately coupled with the detectors. The fundamental unit for this approach is an 8×32 unit cell. We have demonstrated the assembly of the detectors using the PUD geometry to produce a compact, close-packed focal plane array.

REFERENCES

1. Voellmer, G.M. et al. 2003, Proc. SPIE #4855, pp. 63-72; *"Design and fabrication of two-dimensional semiconducting bolometer arrays for HAWC and SHARC-II"*
2. Benford, D.J, Moseley, S.H., Stacey, G.J., Shafer, R.A. & Staguhn, J.G. 2003, Proc. SPIE #4857, pp. 105-114; *"Far-Infrared Imaging Spectroscopy with SAFIRE on SOFIA"*
3. Bradford, C.M. et al. 2002, App. Op. 41, pp. 2561-2575; *"SPIFI: a direct-detection imaging spectrometer for submillimeter wavelengths"*
4. Kosowsky, A. 2003, New. Astron. Rev. #47, pp. 939-943; *"The Atacama Cosmology Telescope"*
5. Nikola, T., Hailey-Dunsheath, S., Stacey, G.J., Benford, D.J., Moseley, S.H. & Staguhn, J.G. 2003, Proc. SPIE #4855, pp. 88-99; *"ZEUS: A Submillimeter Grating Spectrometer for Exploring Distant Galaxies"*
6. Dowell, C.D. et al. 2003, Proc. SPIE #4855, pp. 73-87; *"SHARC II: A Caltech Submillimeter Observatory Facility Camera with 384 Pixels"*; Harper, D.A. et al. 2000, Proc. SPIE #4014, "Airborne Telescope Systems", R.K. Melugin & H.-P. Röser, eds., pp.43-53; *"HAWC: A Far-Infrared Camera for SOFIA"*
7. Irwin, K.D. 1995, Applied Physics Letters 66 (15), pp. 1998-2000, *"An application of electrothermal feedback for high resolution cryogenic particle detection"*
8. Welty, R.P. & Martinis, J.M. 1993, IEEE Trans. On Applied Superconductivity 3 (1), pp.2605-2608, *"Two-stage integrated SQUID amplifier with series array output"*
9. Chervenak, J.A., Irwin, K.D., Grossman, E.N., Martinis, J.M., Reintsema, C.D., & Huber, M.E. 1999, Applied Physics Letters 74 (26), pp.4043-4045, *"Superconducting Multiplexer for Arrays of Transition Edge Sensors"*
10. Grossman, E.N. 1989, "AT-Atmospheric Transmission Software User's Manual, v1.5", Airhead Software Co., 2069 Bluff St., Boulder, CO 80302
11. Voellmer, G.M., Allen, C., Babu, S., Bartels, A., Dowell, C.D., Dotson, J., Harper, D.A., Moseley, S.H. & Smith, W.W. 2004, these proceedings; *"A Two-Dimensional Semiconducting Bolometer Array for HAWC"*
12. Staguhn, J.G., Benford, D.J., Chervenak, J.A., Moseley, S.H., Allen, C.A., Stevenson, T.R. & Hsieh, W.-T. 2004, these proceedings; *"Design Techniques for Improved Noise Performance of Superconducting Transition Edge Sensor Bolometers"*
13. Ullom, J.N. et al. 2004, Appl. Ph. L. #84, pp. 4206-4208; *"Characterization and reduction of unexplained noise in superconducting transition-edge sensors"*
14. Chervenak, J.A. et al. 2004, Nuc. Inst. and Meth. in Phys. Research A, 520, pp. 460-462; *"Fabrication of transition edge sensor X-ray microcalorimeters for Constellation-X"*
15. Benford, D.J. et al. 2000, IJIMW 21 (12), pp. 1909-1916; *"Multiplexed Readout of Superconducting Bolometers"*
16. Holland, W.S., Duncan, W., Irwin, K.D., Walton, A.J., Ade, P.A., & Robson, I. 2003, Proc. SPIE #4855, pp. 1-18; *"SCUBA-2: A New Generation Submillimeter Imager for the James Clerk Maxwell Telescope"*
17. Chervenak, J.A., Benford, D.J, Moseley, S.H., & Irwin, K.D. 2003, in "New Concepts for Far-IR and Submillimeter Space Astronomy", NASA/CP-2003-212233, pp. 378-381; *"Dual Transition Edge Sensor Bolometer for Enhanced Dynamic Range"*
18. Benford, D.J. et al. 1999, ASP Conference series #217, "Imaging at Radio through Submillimeter Wavelengths", p. 134; *"Superconducting Bolometer Arrays for Submillimeter Astronomy"*

19. Staguhn, J.G. et al. 2001, AIP Conference proceedings #605, "Low Temperature Detectors", F.S. Porter et al., eds., pp. 321-324, *"TES Detector Noise Limited Readout Using SQUID Multiplexers"*
20. Benford, D.J. et al. 2000, IJIMW 21 (12), pp. 1909-1916; *"Multiplexed Readout of Superconducting Bolometers"*
21. Benford, D.J. et al. 2001, AIP Conference proceedings #605, "Low Temperature Detectors", F.S. Porter et al., eds., pp. 589-592, *"First Astronomical Use of Multiplexed Transition Edge Bolometers"*
22. Irwin, K.D. et al. 2001, AIP Conference proceedings #605, "Low Temperature Detectors", F.S. Porter et al., eds., pp. 301-304, *"Time-Division SQUID Multiplexers"*
23. Forgione, J., Benford, D.J., Buchanan, E.D., Moseley, S.H., Rebar, J. & Shafer, R.A. 2004, these proceedings; *"Enhancements to a Superconducting Quantum Interference Device (SQUID) multiplexer readout and control system"*
24. Voellmer, G.M. Jackson, M.L., Shirron, P.J. & Tuttle, J.G. 2003, Proc. SPIE #4850, pp. 1070-1079; *"Kinematic Kevlar Suspension System for the HAWC and SAFIRE ADR Salt Pills"*